

AERO2258A Lifting Line Theory Notes

Author: Hadi Winarto

10 May 2004 corrected 19 May 2004

A brief review of CFD for Aerodynamics in general:

It is known that the most complete mathematical model for aeronautical flows is the Navier-Stokes Equations. It is also known that this model is still impossible to try to solve directly (DNS or Direct Numerical Simulation of Navier-Stokes Equation), even using the most advanced numerical methods and the most powerful super computer that exists today. For example, a leading scholar in Computational Aerodynamics, Prof. Jameson of Stanford University, stated the following:

“The complexity of fluid flow is well illustrated in Van Dyke’s Album of Fluid Motion. Many critical phenomena of fluid flow, such as shock waves and turbulence, are essentially nonlinear and the disparity of scales can be extreme. The flows of interest for industrial applications are almost invariably turbulent. The length scale of the smallest persisting eddies in a turbulent flow can be estimated as of order of $1/Re^{3/4}$ in comparison with the macroscopic length scale. In order to resolve such scales in all three spatial dimensions, a computational grid with the order of $Re^{9/4}$ cells would be required. Considering that Reynolds numbers of interest for airplanes are in the range of 10 to 100 million, while for submarines they are in the range of 10^9 , the number of cells can easily overwhelm any foreseeable supercomputer. Moin and Kim reported that for an airplane with 50-meter-long fuselage and wings with a chord length of 5 meters, cruising at 250 m/s at an altitude of 10,000 meters, about 10 quadrillions (10^{16}) grid points are required to simulate the turbulence near the surface with reasonable details. They estimate that even with a sustained performance of 1 Teraflops, it would take several thousand years to simulate each second of flight time. Spalart has estimated that if computer performance continues to increase at the present rate, the Direct Numerical Simulation (DNS) for an aircraft will be feasible in 2075.”

See http://www.stanford.edu/~mfatica/papers/jameson_fatica_hpc.pdf

It is obvious that, at least for the present, the Navier-Stokes Equations must be simplified so that it can be solved numerically using existing computers. If only the large scales turbulence are to be simulated, the Navier Stokes equation can be simplified to become a model which is known as LES or Large Eddy Simulation. This simplified equation is still too difficult to be solved, except for some reasonably simple geometry. LES is still not used in industry, but a lot of research is being carried out in this field.

Further information on LES is given by several authors as follows

“In Large Eddy Simulation the governing equations (the continuity equation, the Navier-Stokes equation, the energy equation etc.) are filtered to separate the large-scale and small-scale turbulence. The large-scale turbulence is solved for by the discretized equations whereas the small-scale turbulence is modelled. Since turbulence is three-dimensional and unsteady, it means that LES must always be carried out as 3D, unsteady simulations.”

See http://www.tfd.chalmers.se/~lada/cfdkurs/cfdkurs02/cfdkurs_2002.html

“Vast increases in the speed and storage capacity of computing machinery and continued development of numerical algorithms demonstrate the progress of computational fluid dynamics (CFD) to provide an effective means for performing design and analysis of aerospace vehicles. While such technical advances are dramatic, the inability of CFD to correctly simulate fluid dynamic turbulence in many situations limits the accurate prediction of performance parameters for practical configurations.

Nonlinear partial differential equations that describe aerodynamic flows and represent the conservation of mass, momentum, and energy provide the basis for CFD. These equations, solved at every point contained in a computational grid and constructed about an air vehicle, employ high-speed computers to provide a simulated flowfield. High-frequency, small amplitude fluctuations of a statistically random nature, commonly referred to as turbulence, often characterize the physical processes of such flows. Researchers typically average the governing equations for practical computations over a time period, which is long compared to the high-frequency oscillations, but may be short with respect to the time it takes air to flow past the vehicle. Thus, researchers do not calculate turbulence properties directly and must modify the equations by incorporating a model to account for their effects. Researchers formulated a substantial number of turbulence models that vary considerably in complexity and in the amount of computational effort required for implementation. Most function reasonably well over a wide range of flow conditions, contributing to the great success of CFD. All turbulence models eventually fail when the fluid state becomes sufficiently intricate and, therefore, cannot accurately predict aerodynamic quantities of interest, such as lift, drag, and heat transfer over general air vehicle configurations, particularly at off-design conditions. In addition, the use of time-averaged flow equations neglects the effects of high-frequency phenomena, which is an important consideration of aero-acoustics, combustion, buffet, flutter, and other fluid-related interactions.

Researchers may compute fine-scale fluid details directly, as an alternate approach to time-averaged equations or traditional turbulence modeling. The designated direct numerical simulation (DNS) procedure places severe requirements on the temporal and spatial resolution of simulated flowfields, resulting in an exorbitant expenditure of computational resources. For this reason, researchers generally limit these calculations to simple geometric configurations. Leaving the smallest turbulent structures spatially under-resolved may extend the utility of DNS. A non-traditional model represents these structures and quantifies only those contributions to the flowfield not supported by the numerical algorithm on the computational grid employed to solve the governing equations. This treatment, referred to as large-eddy simulation (LES), utilizes a subgrid model to indirectly account for the fine-scale turbulent structures. These structures, which are believed to be homogeneous and possess a universal character, may be easily and reliably described.”

See <http://www.afrlhorizons.com/Briefs/Sept01/VA0004.html>

“A large-eddy simulation (LES) code was developed at the NASA Glenn Research Center to provide more accurate and detailed computational analyses of propulsion flow fields. The accuracy of current computational fluid dynamics (CFD) methods is limited primarily by their inability to properly account for the turbulent motion present in virtually all propulsion flows. Because the efficiency and performance of a

propulsion system are highly dependent on the details of this turbulent motion, it is critical for CFD to accurately model it. The LES code promises to give new CFD simulations an advantage over older methods by directly computing the large turbulent eddies, to correctly predict their effect on a propulsion system. Turbulent motion is a random, unsteady process whose behaviour is difficult to predict through computer simulations. Current methods are based on Reynolds-Averaged Navier-Stokes (RANS) analyses that rely on models to represent the effect of turbulence within a flow field. The quality of the results depends on the quality of the model and its applicability to the type of flow field being studied. LES promises to be more accurate because it drastically reduces the amount of modeling necessary. It is the logical step toward improving turbulent flow predictions. In LES, the large-scale dominant turbulent motion is computed directly, leaving only the less significant small turbulent scales to be modeled.”

See <http://www.grc.nasa.gov/WWW/RT2002/5000/5860debonis.html>

Since LES is still not a practical tool for industry, at present the most advanced CFD softwares that are available commercially are all based on RANS or Reynolds Averaged Navier Stokes. In 1895 Osbourne Reynolds (see Houghton and Carpenter Aerodynamics for Engineering Students, 5th edition, page 438) introduced the concept of time (or statistical) averaging and applied the so called Reynolds rules on averaging on the Navier Stokes Equations. The resultant equations are known as the Reynolds Averaged Navier Stokes, which have a fundamental problem known as the Closure problem of turbulence. Basically the problem is that there are more unknown parameters than equations to be solved, such that the system of equation is indeterminate, unless additional equations are introduced. These additional equations are basically empirical in nature and based on what is known as turbulence modelling. Stanford University web site has the following to say about RANS:

“One of the most popular simplifications made to the Navier-Stokes Equations is "*Reynolds Averaging*". This simplification to the full Navier-Stokes equations involves taking time averages of the velocity terms in the equations.

Writing: $u = \langle u \rangle + u'$, $v = \langle v \rangle + v'$, etc. (where $\langle \rangle$ represents a time average) with the fluctuations having zero mean value: $\langle u' \rangle = 0$

we have: $\langle u^2 \rangle = \langle u \rangle^2 + \langle u'^2 \rangle$, $\langle uv \rangle = \langle u \rangle \langle v \rangle + \langle u'v' \rangle$

This allows us to write the time-averaged NS equations as:

$$\rho (\langle u \rangle \langle u_x \rangle + \langle v \rangle \langle u_y \rangle + \langle w \rangle \langle u_z \rangle) = -\langle p_x \rangle + \mu \nabla^2 \langle u \rangle - \rho (\langle u'^2 \rangle_x + \langle u'v' \rangle_y + \langle u'w' \rangle_z)$$

and similarly for the y and z components.

This looks just like the more general Navier Stokes equations for incompressible flow* which hold for steady, laminar flow except that there are additional terms that act as additional stresses on the right hand side. These terms represent the effect of turbulence on the mean flow. They are called "Reynolds stresses" and are sometimes said to be caused by "eddy viscosity". These terms are generally much larger than the normal viscous terms.

The business of predicting these stresses and relating them to the computed mean flow properties is called turbulence modeling. This is usually accomplished empirically or by using the results of detailed time-dependent simulations.

Reynolds averaged NS solvers are appropriate for the analysis of viscous, compressible flows and have been applied to rather general configurations, but one

must be careful that the assumptions of the turbulence model are compatible with the characteristics of the flow of interest.”

See <http://adg.stanford.edu/aa208/modeling/rans.html>

See also <http://aerodyn.org/CFD/NSE/nse.html>

And also <http://www.le.ac.uk/engineering/ar45/eg7029/eg7029w/node38.html>

There are quite a few RANS based CFD softwares that are available commercially, such as POLYFLOW, CFX , FIDAP, FLOTRAN, PHOENICS, CFX, STAR-CD, FLUENT etc. For complex geometries, the computer run times for these programs are usually very long if done on a PC. Industrial type problems are usually run on specialized work-stations or clustered super computers.

Even though RANS based softwares have been available since the 1990s, for routine calculations an aerospace company usually uses Euler equation based softwares. The Euler solver assumes that the flow is inviscid. For most calculations, except for predicting drag, the Euler solver is usually sufficiently accurate. The run time for an Euler solver is very much faster than for a RANS solver, when solving the same problem. The Euler solver was still very much a research tool before the 1980s, when the most common tool used in Aerospace industries was Full Potential Equation (FPE) solver. The FPE can be obtained from the Euler equation by making the simplifying assumption that the flow is irrotational. Shock waves are basically rotational, but FPE was able to capture shock waves that were not too strong, by some clever numerical manipulations.

Prior to the late 1970s most advanced computational aerodynamic softwares were based on simplified version of the FPE, known as the Transonic Small Disturbance (TSD) or Transonic Small Perturbation (TSP). The simplification is obtained by assuming that the wing or aerofoil is very thin.

Further simplifications can be obtained by assuming that the flow is incompressible (as well as being inviscid and irrotational). For this type of flow the governing equation is known as the Potential Equation or the Laplace equation, which can be solved using a number of techniques, all of which are based on the linearity property of the Laplace equation. The Laplace equation has a number of elementary solutions, which can be used as building blocks for solving the aerodynamic problem. For 3-D flows, the problem can be solved using the panel method, the vortex lattice method and the Lifting Line Theory etc. For 2-D flows, the aerodynamic problem based on the Laplace equation can be solved using the panel method and the Complex Variable Conformal Mapping method. If the wing is assumed to be very thin and very lightly cambered then the 2-D problem can be solved using the Thin Aerofoil Theory, while the 3-D problem can be solved using the Lifting Line Theory (LLT)

This lecture note will discuss the Lifting Line Theory in greater details, while the Thin Aerofoil Theory (TAT) has been discussed previously elsewhere.

Finite span wing of constant cross section.

According to the thin aerofoil theory (TAT), the slope of the lift coefficient versus angle of attack curve for an infinitely long aerofoil has a value of 2π . An aerofoil by definition is a 2-D wing whose cross section is exactly the same all along the span. In reality obviously there is no such thing as an infinitely long aerofoil. All aerofoils must be of finite length. The ratio of the span length of the aerofoil to its chord length is called the aspect ratio (AR). Wind tunnel testing has shown that a finite length aerofoil has a lift to angle of attack curve slope of less than 2π . The value of the

slope becomes smaller as the aspect ratio is reduced. This is in contradiction to the prediction of TAT and is caused by 3-D effect, which we must now study.

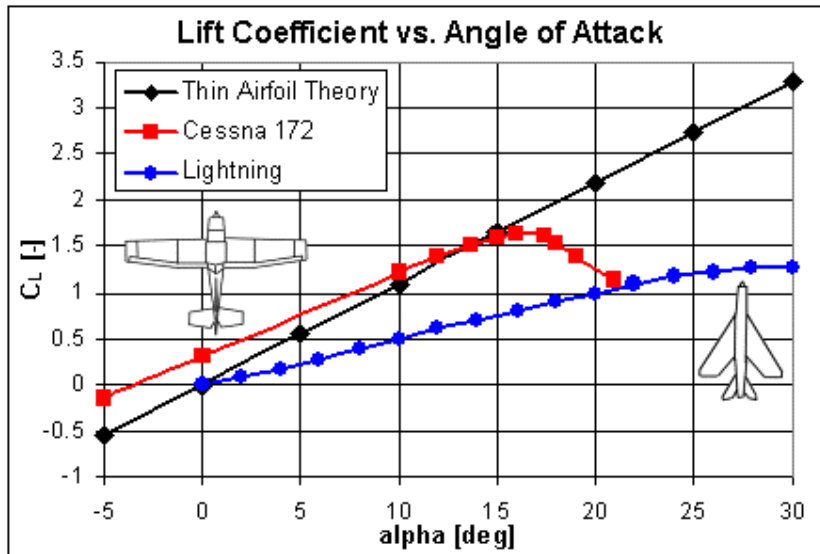


Fig.1 Lift curve slope varies as a function of aspect ratio
(Obtained from <http://www.aerospaceweb.org/question/aerodynamics/q0167.shtml>)

Firstly, it must be remembered that in TAT the infinitely long aerofoil is replaced by a vortex panel, which is infinitely long and normal to the plane of the page. If the aerofoil is of finite length, then each vortex filament, which makes up the vortex sheet, must be of finite length also, namely as long as the wing's span. However, we know from Kelvin-Helmholtz theorem of vortex motion (e.g. see page 215 of Houghton and Carpenter 5th ed) that a vortex filament can't end in a fluid. A vortex must be infinitely long, or must form a close loop or ends on a solid boundary. It is obvious that we can't represent the finite length aerofoil by a bunch of finite length vortex along the span of the wing. The vortex filament must be infinitely long or forming a closed loop. This problem can be resolved as follows. When an aircraft starts to move along the runway, a starting vortex is generated along the span of the wing, which is then shed and remains fixed at the runway (e.g. see Houghton and Carpenter 5th ed page 211). Since initially the flow around the wing is irrotational, therefore the circulation of the system must also be zero. Since vorticity or circulation can't be created therefore the total circulation must remain zero with time. This means that to counteract the circulation around the starting vortex, a new vortex must be created along the wing span but in the opposite direction such that the total vorticity remains zero. The starting vortex is connected to the vortex, which is bound on the wing, by 2 vortex filaments, each of which begins at each wing tip. The moving wing is then represented by a closed loop in the form of a rectangle. However, after a sufficiently long time the bound vortex on the wing would have moved very far away from the starting vortex, such that the effect of the starting vortex on the airflow around the wing can be neglected. In other words, instead of a rectangular shape vortex filament, we now have a U shape or horseshoe shape vortex filament to represent the moving finite length wing (see Houghton and Carpenter page 214). The short base of the U is located at the quarter chord line of the wing, whereas the two wing tip vortices, which forms the sides of the U, are semi infinitely long.

When a wing is moving through a stationary air, or conversely when a large body of air (e.g. in a wind tunnel) moves uniformly over a stationary wing, the shape of the aerofoil is such that the air moves faster over the upper part of the wing when compared to the air that moves under the lower part of the wing. This implies that the pressure over the upper part is less than the pressure under the lower part of the wing. Since air tends to flow from the high pressure to a lower pressure region, therefore there is a tendency for air to try to move from the lower part to the upper part of the wing. However, the wing is made of solid material and obviously no air particle can penetrate into the wing and moves from the lower to the upper part of the wing, except at the wing tip, where air is free to move from the lower to the upper part of the wing. The direction of air motion is span-wise. On the upper part air moves from the tip to the root of the wing, whereas along the lower part air moves from the wing root towards the tip region. It can be easily understood then, that the flow over the finite length wing is not truly 2-dimensional, since there is a cross flow along the span-wise direction.

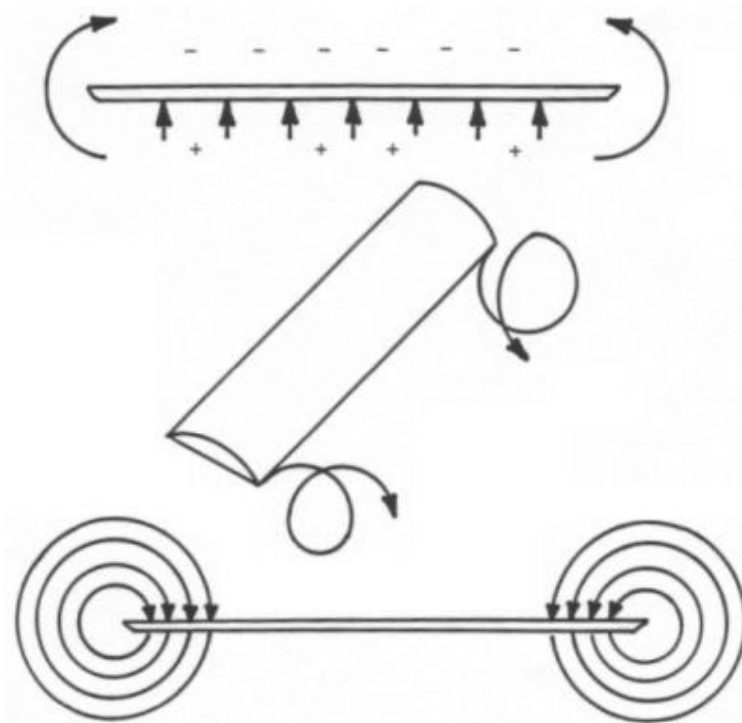


Fig. 2 Span-wise flow on a finite length wing causes trailing vortices to be formed.
 (Obtained from <http://www.aerospaceweb.org/question/aerodynamics/q0167.shtml>)

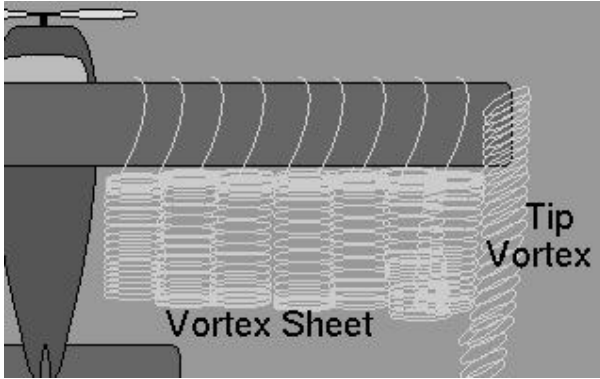


Fig. 3 Trailing vortex sheet is shed by the wing.
 (Obtained from <http://www.adl.gatech.edu/classes/lowspd aero/lospd1/lospd1.html>)

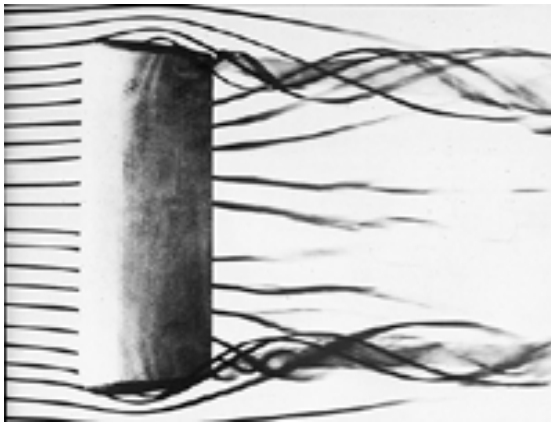


Fig. 4 The initially straight streamlines upstream of the finite wing become rotational after flowing over the wing, creating vorticity.
 From <http://www.desktopaero.com/appliedaero/potential3d/finitewings.html>

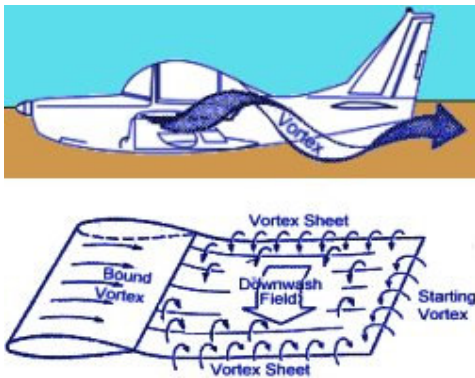


Fig. 5 Formation of the starting vortex and generation of the horseshoe vortex.
 (Obtained from <http://www.pilotsweb.com/principle/liftdrag.htm>)

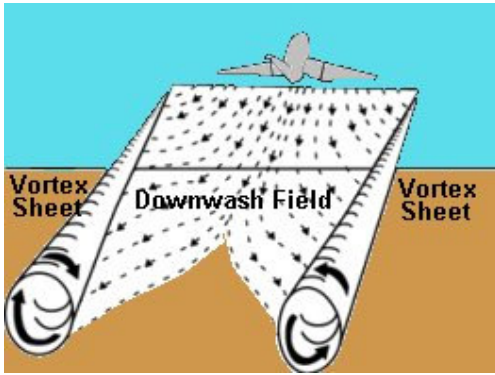


Fig. 6 Vortex sheet shed by the wing
(Obtained from <http://www.pilotsweb.com/principle/liftdrag.htm>)

It is to be expected, however, that the cross flow velocities involved would be very much smaller than the longitudinal (forward motion) velocity of the aircraft's wing. Thus it is quite reasonable to assume that the main flow is basically still 2-D. By assuming that the flow is locally 2-D, we can evaluate the aerodynamic properties of the wing as being the linear sum of the elemental aerofoils making up the wing. The very difficult 3-D problem can then be reduced in its complexity to become the much simpler 2-D problem. However, as noted earlier (see fig. 1) the lift curve slope of a finite wing is less than that for the infinite aerofoil, which is predicted using 2-D assumption. This difficulty can be resolved by noting the fact that horseshoe vortices are shed from the trailing edge of the wing. Each horseshoe vortex would induce a downward velocity at the wing, thus the angle of attack of the airflow seen by the wing is somewhat less than the geometric angle of incidence of the wing.

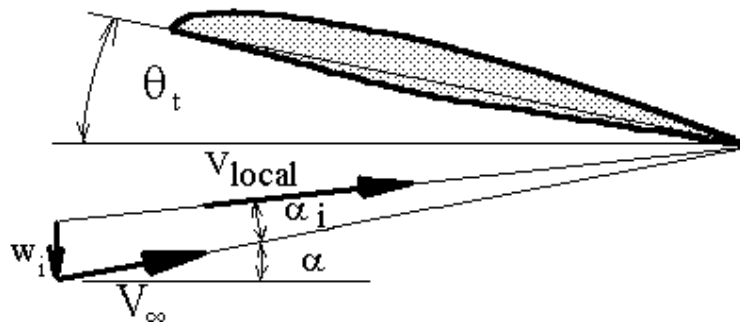


Fig. 7 Downward air velocity induced by trailing vortices decreases the angle of attack seen by the local aerofoil section.
(Obtained from <http://www.ae.su.oz.au/aero/liftline/liftline.html>)

As can be seen from the above figure, the direction of airflow approaching the wing is not the free stream direction (indicated by the vector V_∞) but by the local velocity vector, V_{local} . The angle of incidence seen by the aerofoil is thus the local angle of incidence, which is the free stream angle α less the downwash angle α_i . Because the effective angle of incidence is reduced, the lift generated by the elemental aerofoil would be less than if the flow is truly 2-D without any vorticity being shed at the

trailing edge. Since the downwash angle always reduces the effective angle of incidence all along the span, therefore the overall lift generated by the wing would also be less than that predicted by a 2-D method. This is the reason why the lift curve slope of a finite wing is less than that which would be produced by a truly 2-D wing. Furthermore, it is logical to think that the effect of the cross flow would be felt more strongly along the span if the aspect ratio is smaller, hence the slope of the lift curve would be smaller for smaller value of aspect ratio.

It should also be noted that the actual lift produced by an elemental aerofoil acts along a line normal to the local velocity vector, and not normal to the free stream vector. On the other hand, without considering the local situation lift is always defined as the force, which is normal to the direction of the free stream, whereas the force component along the free stream direction, thus opposing the motion, is called drag. The actual elemental lift produced by the local aerofoil can be resolved into 2 components. One of the force components is along the direction normal to the free stream direction, and the other is along the free stream direction. The force component normal to the free stream direction is obviously the elemental lift, but now surprisingly we have a drag component along the direction of the free stream, even though the flow is assumed to be inviscid. Furthermore, the drag produced is equal to the lift multiplied by $\sin \alpha_i$. For small angles we have $\sin \alpha_i \approx \alpha_i$, thus the drag is equal to lift multiplied by downwash angle. Since the drag is created by the presence of induced velocity caused by the trailing vortex, therefore it is referred to as induced drag. Since it is always present whenever a wing produces lift, it is also referred to as lift dependent drag. When lift is zero, the induced drag is also zero.

The distribution of the horseshoe vortices on the finite wing can be seen in figure 5.21 on page 231 of Houghton and Carpenter 5th ed. If the short base of each U vortex filament is assumed to be located at the quarter chord point of the wing, then aerodynamically speaking the wing can be modelled as a bound vortex along the quarter chord line plus an infinite number of trailing vortex filaments which can be said to form a trailing vortex sheet (see fig. 8 below)

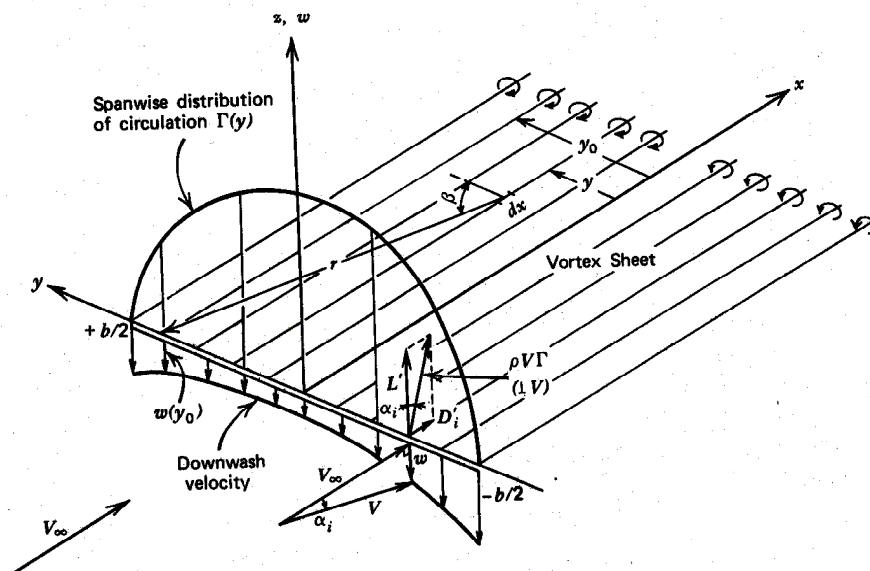


Fig. 8 Bound vortex and trailing vortex sheet, representative of a finite wing.
(Obtained from : http://cromagnon.stanford.edu/aa200b/lect_notes/lect13-14.pdf)

From the Kelvin-Helmholtz theorem it is known that the strength of any vortex filament is constant along its length. However, the bound vortex is not really a vortex filament, but more like a vortex tube consisting of an infinite number of filaments of varying lengths, the longest being about the same as the span of the wing and the shortest having a length approaching zero (this is for the U vortex filament, which is located along the midpoint of the span). Keeping this in mind, we can now say that the strength of the bound vortex tube varies along the span of the wing. If the midpoint of the wing span is taken to be the origin of the y-axis, then the strength of the bound vortex is a function of y, the distance from the origin to a point along the wing span. The port wing tip is located at $y = -b/2$ whereas the starboard wing tip is located at $y = +b/2$, where b is the span length of the wing. If the vortex strength at y is $\Gamma(y)$ and the strength at $y+\Delta y$ is $\Gamma(y+\Delta y) = \Gamma(y) + \Delta\Gamma(y)$, then the strength of the trailing filament at y is obviously equal to $\Delta\Gamma(y)$, which is also equal to

$$\Gamma'(y).dy, \text{ where } \Gamma'(y) = \frac{d\Gamma(y)}{dy}.$$

Let us now consider the induced velocity at point y^* somewhere along the span of the wing. The induced velocity at y^* due to the bound vortex is zero, since a straight vortex can't induce a velocity on itself. However, the semi infinitely long trailing vortex filament at y, the strength of which is $\Delta\Gamma(y)$, would induce a downward velocity the magnitude of which is given by the Biot-Savart rule as follows (e.g. see page 218 of Houghton and Carpenter 5th ed)

$$dw = -\frac{\Delta\Gamma(y)}{4\pi(y^*-y)} = -\frac{\Gamma'(y).dy}{4\pi(y^*-y)} \quad (1)$$

The total induced velocity at y^* is then given by

$$w(y^*) = -\frac{1}{4\pi} \int_{-b/2}^{b/2} \frac{\Gamma'(y).dy}{(y^*-y)} \quad (2)$$

From fig.7 it can be seen that the induced downwash angle is given as follows

$$\alpha_i \approx \tan^{-1}\left(\frac{-w}{V_\infty}\right) = \frac{1}{4\pi V_\infty} \int_{-b/2}^{b/2} \frac{\Gamma'(y).dy}{(y^*-y)} \quad (3)$$

The effective angle of attack at y^* is

$$\alpha_{eff}(y^*) = \alpha(y^*) - \alpha_i(y^*) \quad (4)$$

If the aerofoil is cambered and its zero lift angle of attack is α_0 , then the effective angle of attack becomes

$$\alpha_{eff}(y^*) = \alpha(y^*) - \alpha_i(y^*) - \alpha_0(y^*) \quad (5)$$

Note that α_0 is always negative for a normally cambered aerofoil.

From the 2-D potential flow theory we know that the lift coefficient is given by

$$C_l = 2\pi.\alpha_{eff} = 2\pi(\alpha - \alpha_i - \alpha_0) \quad (6)$$

The lift produced by an elemental aerofoil of width dy^* at y^* is then

$$Lift = \frac{1}{2} \rho V_\infty^2 . c dy^* . C_l (y^*) = \pi \rho V_\infty^2 c dy^* . (\alpha - \alpha_i (y^*) - \alpha_0)$$

where c is the aerofoil's chord length and C_l is its lift coefficient, whereas ρ and V_∞ are air density and free stream velocity respectively.

Now from the Kutta-Joukowski lift theorem, we know that for the elemental aerofoil

$$Lift = \rho V_\infty \Gamma (y^*) dy^*$$

therefore

$$\rho V_\infty . \Gamma (y^*) = \pi \rho V_\infty^2 c . (\alpha - \alpha_i (y^*) - \alpha_0) \quad (7)$$

The above equation can be simplified as follows

$$\frac{\Gamma (y^*)}{\pi V_\infty c} + \alpha_i (y^*) = \alpha - \alpha_0$$

Substitution of equation (3) into the above equation gives the following result

$$\frac{\Gamma (y^*)}{\pi V_\infty c} + \frac{1}{4\pi V_\infty} \int_{-b/2}^{b/2} \frac{\Gamma' (y) . dy}{(y^* - y)} = \alpha - \alpha_0 \quad (8)$$

The above equation must be satisfied at all points y^* along the span.

Since the distribution of vortex tube strength, $\Gamma (y^*)$, is smooth and continuous, and may be symmetric (when the ailerons are undeflected) or antisymmetric (when the ailerons are deflected, such as when the aircraft is turning), it is suitable to represent the unknown solution as a Fourier series, with unknown constants.

Let us assume that the solution can be satisfactorily approximated by the following Fourier series

$$\Gamma (y) = 2b V_\infty \sum_{n=1}^{\infty} A_n \sin n\theta \quad (9)$$

It should now be noted that

$$\Gamma' (y) . dy = \frac{d\Gamma (y)}{dy} . dy = \frac{d\Gamma (\theta)}{d\theta} . d\theta \quad (10)$$

Therefore

$$\Gamma'(y).dy = 2bV_\infty \sum_{n=1}^{\infty} nA_n \cos n\theta.d\theta \quad (11)$$

The polar coordinate, θ , is related to the Cartesian coordinate, y , as follows

$$y = -\frac{b}{2} \cos \theta \quad (12)$$

The relationship should satisfy the requirements that when $y = -b/2$ then $\theta = 0$, while when $y = +b/2$ then $\theta = \pi$. It can be easily shown that equation (12) indeed satisfies the above requirements.

Now it should be noted that

$$y^* - y = \frac{b}{2} (\cos \theta - \cos \theta^*) \quad (13)$$

Now equation (8) can be rewritten as follows

$$\frac{2bV_\infty \sum_{n=1}^{\infty} A_n \sin n\theta^*}{\pi V_\infty c} + \frac{1}{4\pi V_\infty} \frac{2bV_\infty \sum_{n=1}^{\infty} n.A_n \int_0^\pi \frac{\cos n\theta.d\theta}{(\cos \theta - \cos \theta^*)}}{\frac{1}{2}b} = \alpha - \alpha_0 \quad (14)$$

From basic mathematical theory, it is known that

$$\int_0^\pi \frac{\cos n\theta}{(\cos \theta - \cos \theta^*)} d\theta = \pi \frac{\sin n\theta^*}{\sin \theta^*} \quad (15)$$

Equation (14) can now be simplified to become

$$\frac{2b}{\pi c} \sum_{n=1}^{\infty} A_n \sin n\theta^* + \sum_{n=1}^{\infty} n.A_n \cdot \frac{\sin n\theta^*}{\sin \theta^*} = \alpha - \alpha_0 \quad (16)$$

Theoretically speaking the above equation must be satisfied at every point y^* along the wing span, so that we have an infinite number of equations to be solved simultaneously to calculate the infinite number of unknown Fourier constants (amplitudes), A_n . This is obviously not very practical, if not impossible to do. In practice equation (16) is required to be satisfied at a few points on the wing span. Equation (16) is now replaced by the following

$$\frac{2b}{\pi c} \sum_{n=1}^N A_n \sin n\theta^* + \sum_{n=1}^N n.A_n \cdot \frac{\sin n\theta^*}{\sin \theta^*} = \alpha - \alpha_0 \quad (17)$$

where N is a reasonably large number, around 20 or less, of points on the wing span at which the equation must be satisfied.

The approximation for the bound vortex tube strength distribution, i.e. equation (9), must now be modified slightly as follows

$$\Gamma(\theta^*) = 2bV_\infty \sum_{n=1}^N A_n \sin n\theta^* \quad (18)$$

For a symmetric distribution of lift along the wing span, the lift distribution along the right (starboard side) wing is a mirror image of the distribution along the left (port side) wing. For such a situation it is only necessary to calculate the lift distribution on one side of the wing span only. This will reduce the number of points at which the equation (17) must be satisfied by half.

If N is an even number, $N = 2M$, equation (18) can be replaced as follows

$$\Gamma(\theta^*) = 2bV_\infty \left[\sum_{m=1}^M A_{2m-1} \sin(2m-1)\theta^* + \sum_{m=1}^M A_{2m} \sin 2m\theta^* \right] \quad (19)$$

On the other hand if N is odd, $N = 2M + 1$, equation (18) can be replaced by

$$\Gamma(\theta^*) = 2bV_\infty \left[\sum_{m=1}^{M+1} A_{2m-1} \sin(2m-1)\theta^* + \sum_{m=1}^M A_{2m} \sin 2m\theta^* \right] \quad (20)$$

Let us now consider 2 points on the wing, each being a mirror image of the other. In other words, if one of the points is the point θ^* , where $0 < \theta^* < \pi/2$, the other point is the point $\pi - \theta^*$. The application of equation (19) at point $\pi - \theta^*$ would give the following results

$$\Gamma(\pi - \theta^*) = 2bV_\infty \left[\sum_{m=1}^M A_{2m-1} \sin(2m-1)(\pi - \theta^*) + \sum_{m=1}^M A_{2m} \sin 2m(\pi - \theta^*) \right]$$

Now it should be noted that

$$\sin(2m-1)(\pi - \theta^*) = \sin(2m-1)\theta^*$$

$$\sin 2m(\pi - \theta^*) = -\sin 2m\theta^*$$

Therefore

$$\Gamma(\pi - \theta^*) = -2bV_\infty \left[\sum_{m=1}^M A_{2m-1} \sin(2m-1)\theta^* - \sum_{m=1}^M A_{2m} \sin 2m\theta^* \right] \quad (21)$$

Due to symmetry we must have $\Gamma(\theta^*) = \Gamma(\pi - \theta^*)$ or

$$\begin{aligned} \sum_{m=1}^{M+1} A_{2m-1} \sin(2m-1)\theta^* + \sum_{m=1}^M A_{2m} \sin 2m\theta^* \\ = \sum_{m=1}^M A_{2m-1} \sin(2m-1)\theta^* - \sum_{m=1}^M A_{2m} \sin 2m\theta^* \end{aligned} \quad (22)$$

It can be clearly seen that equation (22) can only be satisfied if all even terms of the Fourier amplitudes, A_{2m} , must be zero. Therefore, both equations (19) and (21) are now the same equation given by

$$\Gamma(\theta^*) = \Gamma(\pi - \theta^*) = 2bV_\infty \sum_{m=1}^M A_{2m-1} \sin(2m-1)\theta^* \quad (23)$$

If it is now defined that

$$\bar{A}_m = A_{2m-1} \quad \text{for } m = 1, 2, 3, \dots, M. \quad (24)$$

then equation (23) can be written in a slightly different form as follows

$$\Gamma(\theta^*) = \Gamma(\pi - \theta^*) = 2bV_\infty \sum_{m=1}^M \bar{A}_m \sin(2m-1)\theta^* \quad (25)$$

It can be shown by following the same argument that if N is odd, which means that the wing's mid span point is chosen as one of the control points, then we have

$$\Gamma(\theta^*) = \Gamma(\pi - \theta^*) = 2bV_\infty \sum_{m=1}^{M+1} \bar{A}_m \sin(2m-1)\theta^* \quad (26)$$

The above discussion shows that for a symmetric wing load distribution we need to compute only the odd numbered Fourier coefficients, thus the number of equations to be solved simultaneously is reduced to only half of the more general situation, which is represented by equation (17) applied at N distinct control points. It is also logical to select N to be an even number so that $N = 2M$, even though an odd value of N is also permissible. For the same amount of computational effort an even value of N gives a better accuracy than an odd value of N. In the following discussion we will assume that N is even.

For a symmetric wing loading condition, and the choice of the index N being even so that $N = 2M$, the governing equation is a simplified form of equation (17) as follows

$$\frac{2b}{\pi c} \sum_{m=1}^M \bar{A}_m \sin(2m-1)\theta^* + \sum_{m=1}^M (2m-1) \bar{A}_m \frac{\sin(2m-1)\theta^*}{\sin \theta^*} = \alpha - \alpha_0 \quad (27)$$

Now let us define the following

$$C_m^* = \left(\frac{2b}{\pi c} + \frac{(2m-1)}{\sin \theta^*} \right) \sin(2m-1)\theta^* \quad (28)$$

Equation (27) can now be written in a more compact and familiar form as follows

$$\sum_{m=1}^M C_m^* \bar{A}_m = \alpha - \alpha_0 \quad (29)$$

The distribution of the bound vortex strength as given by equation (25) requires that we solve an MxM simultaneous equations, i.e. equation (29) applied M times at M distinct control points on one side only of the wing. The control points may be chosen as follows. The left half of the wing span is divided up into M equal intervals, which is equivalent to dividing up the whole span into N equal intervals, and the control points are chosen to be the midpoints of the intervals so that their coordinates are given by the following equation

$$y_k = -\frac{b}{2} \left(1 - \frac{2k-1}{2M} \right) \quad \text{for } k=1, 2, 3, \dots, M \quad (30)$$

The polar coordinates corresponding to the control points are then calculated as follows

$$\theta_k = \cos^{-1} \left(-\frac{2}{b} y_k \right) = \cos^{-1} \left(1 - \frac{2k-1}{2M} \right) \quad \text{for } k=1, 2, \dots, M \quad (31)$$

The system of equations that must be solved numerically is now given by

$$\sum_{m=1}^M C_{km} \bar{A}_m = \alpha - \alpha_0 \quad \text{for } k=1, 2, 3, \dots, M \quad (32)$$

where the matrix coefficients C_{km} is given by equation (28) applied at the point y^* , which is represented by the k^{th} control point or for $\theta^* = \theta_k$

$$C_{km} = \left(\frac{2b}{\pi c} + \frac{(2m-1)}{\sin \theta_k} \right) \sin(2m-1)\theta_k \quad \text{for } m=1, 2, 3, \dots, M \quad (33)$$

The system of simultaneous equations (32) can be solved to give the values of the Fourier coefficients \bar{A}_m , for $m = 1, 2, \dots, M$, which are then used in the formula for the sought for solution of the bound vortex strength distribution as follows

For any value of y between the range of $-b/2 < y < 0$ and $\theta = \cos^{-1} \left(-\frac{2y}{b} \right)$ the values of the local bound vortex strength at y and at $-y$, are given by the following equation

$$\Gamma(y) = \Gamma(-y) = \Gamma(\theta) = 2bV_\infty \sum_{m=1}^M \bar{A}_m \sin(2m-1)\theta \quad (34)$$

The load or lift per unit length distribution along the span is given by the following

$$\Delta L(y) = \Delta L(-y) = \Delta L(\theta) = \rho V_\infty \Gamma(\theta) = 2b\rho V_\infty^2 \sum_{m=1}^M \bar{A}_m \sin(2m-1)\theta \quad (35)$$

Therefore the total lift acting on the wing, which is twice that of the lift on the semi-span only, is thus given by the following equation

$$Lift = 2 \int_{-b/2}^0 \Delta L(y).dy = 2 \int_{-b/2}^0 \Delta L(y) \cdot \frac{dy}{d\theta} \cdot d\theta = 2 \frac{b}{2} \int_0^{\pi/2} \Delta L(y) \cdot \sin \theta \cdot d\theta$$

$$Lift = 2b^2 \rho V_\infty^2 \sum_{m=1}^M \bar{A}_m \int_{-b/2}^0 \sin(2m-1)\theta \cdot \sin \theta \cdot d\theta$$

Now we know that $\int_0^{\pi/2} 2 \sin \theta \cdot \sin \theta \cdot d\theta = \int_0^{\pi/2} (1 - \cos 2\theta) d\theta = \frac{\pi}{2}$ and for $m \neq 1$ we also know that $2 \sin(2m-1)\theta \cdot \sin \theta = \cos((2m-2)\theta) - \cos(2m\theta)$, therefore for $m \neq 1$

$$2 \int_0^{\pi/2} \sin(2m-1)\theta \cdot \sin \theta \cdot d\theta = \int_0^{\pi/2} [\cos((2m-2)\theta) - \cos(2m\theta)] \cdot d\theta = 0 \quad (36)$$

The total lift on the wing is then

$$Lift = \frac{1}{2} \pi b^2 \rho V_\infty^2 \bar{A}_1 \quad (37)$$

Therefore the lift coefficient for the wing is given by

$$C_L = \frac{Lift}{\frac{1}{2} \rho V_\infty^2 \cdot S} = \pi \cdot AR \cdot \bar{A}_1 \quad (38)$$

where S is the wing area and AR is the Aspect Ratio of the wing

$$S = b \cdot c \quad (39)$$

$$AR = \frac{b^2}{S} = \frac{b}{c} \quad (40)$$

It should be remembered that the result obtained above is based on the assumption that the local flow around each elemental aerofoil is 2-dimensional. This assumption is obviously not very accurate, because we know that there is a cross flow along the wing span. If the aspect ratio of the wing is quite large, then the cross flow would be felt most strongly only near the tip region, whereas everywhere else along the wing span the 2-dimensional flow assumption should be quite appropriate. However, if the aspect ratio is small, then the cross flow would be felt all along the wing span and the 2-dimensional flow assumption would be erroneous throughout most of the wing span. It follows, therefore, that the result obtained above should be valid for any wing with fairly large aspect ratio, but the result would become more and more erroneous as the aspect ratio of the wing is decreased.

It was stated earlier (see page 8) that the direction of airflow approaching the wing is not the free stream direction (indicated by the vector V_∞) but the direction of the local velocity vector, V_{local} , which varies along the span. The change in the local velocity direction is caused by the induced velocity, and is given by the induced angle, the magnitude of which is given by equation (3). The presence of induced angle is the source of the creation of the induced drag.

Let C_{di}^* be the local induced drag coefficient, and its magnitude is then given by

$$C_{di}^* = C_l^* \cdot \tan \alpha_i^* \approx C_l^* \cdot \alpha_i^* \quad (41)$$

The total induced drag acting on the wing can be obtained by integrating the above local drag expression for all values of y along the wing span

$$C_{Di} = \frac{1}{b} \int_{-b/2}^{b/2} C_l^*(y^*) \cdot \alpha_i^*(y^*) \cdot dy^* = \frac{1}{2} \int_0^\pi C_l^*(\theta^*) \cdot \alpha_i^*(\theta^*) \cdot \sin \theta^* d\theta^* \quad (42)$$

The local induced downwash angle is given by equation (3) shown on page 10, where the strength of the trailing vortex element is given by equation (11). The integral of equation (3) has actually been evaluated (see equation (14)) and can be written more explicitly as follows.

$$\alpha_i^* = \frac{2bV_\infty}{4\pi V_\infty \frac{1}{2}b} \sum_{n=1}^N n \cdot A_n \int_0^\pi \frac{\cos n\theta \cdot d\theta}{(\cos \theta - \cos \theta^*)} = \sum_{n=1}^N n \cdot A_n \cdot \frac{\sin n\theta^*}{\sin \theta^*} \quad (43)$$

The local lift coefficient, at y^* , can be evaluated as follows

$$C_l^* = \frac{\rho V_\infty \Gamma^*}{\frac{1}{2} \rho V_\infty^2 c} = \frac{2\Gamma^*}{V_\infty c} = \frac{4b}{c} \sum_{n=1}^N A_n \sin n\theta^* \quad (44)$$

Equation (42) can now be processed further as follows

$$C_{Di} = \frac{2b}{c} \int_0^\pi \sum_{k=1}^N A_k \sin k\theta^* \cdot \sum_{n=1}^N n \cdot A_n \cdot \frac{\sin n\theta^*}{\sin \theta^*} \sin \theta^* d\theta^*$$

$$C_{Di} = \frac{2b}{c} \sum_{k=1}^N \sum_{n=1}^N n \cdot A_n \cdot A_k \int_0^\pi \sin n\theta^* \cdot \sin k\theta^* d\theta^*$$

Now we know that

$$\int_0^\pi \sin n\theta \cdot \sin k\theta \cdot d\theta = 0 \text{ for } n \neq k$$

$$\int_0^\pi \sin n\theta \cdot \sin n\theta \cdot d\theta = \frac{\pi}{2n} \text{ for } n = k$$

Therefore

$$C_{Di} = \frac{\pi b}{c} \cdot \sum_{n=1}^N n \cdot A_n^2 = \pi \cdot AR \cdot A_1^2 \sum_{n=1}^N n \cdot \left(\frac{A_n}{A_1} \right)^2$$

$$C_{Di} = \frac{(\pi \cdot AR \cdot A_1)^2}{\pi \cdot AR} \sum_{n=1}^N n \cdot \left(\frac{A_n}{A_1} \right)^2 = \frac{C_L^2}{\pi \cdot AR} \sum_{n=1}^N n \cdot \left(\frac{A_n}{A_1} \right)^2$$

Now let us define the following quantity, e.

$$e = \frac{1}{\sum_{n=1}^N n \cdot \left(\frac{A_n}{A_1}\right)^2} = \frac{1}{1 + \sum_{n=2}^N n \cdot \left(\frac{A_n}{A_1}\right)^2} \quad (45)$$

thus

$$C_{Di} = \frac{C_L^2}{\pi \cdot AR \cdot e} \quad (46)$$

The quantity e as defined above is known as the Oswald efficiency factor. (e.g. see <http://www.rmcs.cranfield.ac.uk/aerextra/olaedrag.ppt>)

It can be seen from equation (45) that the Oswald efficiency factor is always less than 1. The maximum value of e = 1 is obtained for the special case of wing load distribution given by equation (9) where $A_n = 0$ for all values of n, except for n = 1.

This special load distribution is then given by the following equation

$$\Gamma(y) = \Gamma(\theta) = 2bV_\infty \sum_{n=1}^{\infty} A_n \sin n\theta = 2bV_\infty A_1 \sin \theta$$

Since $\cos \theta = -\frac{2y}{b}$ therefore $\sin \theta = \sqrt{1 - \left(\frac{2y}{b}\right)^2}$ and the span wise distribution of wing load is given by

$$\Gamma(y) = 2bV_\infty A_1 \sqrt{1 - \left(\frac{2y}{b}\right)^2} \quad (47)$$

and also

$$c \cdot C_l(y) = \frac{2\Gamma}{V_\infty} = 4bA_1 \sqrt{1 - \left(\frac{2y}{b}\right)^2} \quad (48)$$

Since $4bA_1$ is a constant therefore the wing load distribution that has the best value of Oswald efficiency of e = 1, is the elliptic distribution as shown above.

It should be noted that the function $f = \sqrt{1 - \left(\frac{2y}{b}\right)^2}$ can be rewritten as

$$f^2 + \left(\frac{2y}{b}\right)^2 = 1$$

, which is the equation of an ellipse, with a major axis of b/2 along the y-axis and a minor axis of 1 along the f-axis normal to y.

Equation (48) shows that the elliptic load distribution can be obtained for a wing with constant aerofoil section, C_l , provided that the chord length of the wing has an elliptical span wise distribution. The Spitfire was a famous World War II fighter that had an elliptical planform, thus an elliptical distribution of span wise chord length. Further interesting information about the Spitfire can be gleaned from the following web sites

<http://142.26.194.131/aerodynamics1/Drag/Page6.html>
http://www.odyssey.dircon.co.uk/Spitfire_dev.htm
http://www.centennialofflight.gov/essay/Theories_of_Flight/Reducing_Induced_Drag/TH16.htm
<http://www.glide.dyndns.org/on-the-wing4/>

The tooling and other costs involved in the manufacture of elliptical wing were not and still not economical, thus the elliptical wing is no longer considered for production purposes.

Tapered and Twisted Finite Wing

It should be noted, however, that a simpler planform shape that is much easier and cheaper to manufacture, such as a simple tapered wing can be selected to give an almost elliptical wing load span wise distribution and thus minimizing the associated induced drag. Furthermore, equation (48) shows that even a rectangular wing can be designed to have an almost elliptical lift distribution by suitably varying the aerofoil or sectional shape and its local geometric angle of incidence (by twisting the wing), i.e. varying the span wise distribution of either or both α and α_0 , such that the local lift coefficient distribution, $C_l(y)$, approaches an elliptical distribution.

Now it should be noted that equation (45) was derived without recourse to the possibility of simplifying the problem by taking advantage of the possibility that the lift distribution may be symmetrical. If the lift distribution is symmetrical, it was shown earlier that all the even numbered Fourier amplitudes are all zero. This means that the Oswald efficiency factor for a symmetrical lift distribution is given by

$$e = \frac{1}{\sum_{n=1}^{N/2} (2n-1) \cdot \left(\frac{\bar{A}_n}{\bar{A}_1}\right)^2} = \frac{1}{1 + \sum_{n=2}^{N/2} (2n-1) \cdot \left(\frac{\bar{A}_n}{\bar{A}_1}\right)^2} \quad (49)$$

where \bar{A}_n for $n = 1, 2, \dots, N/2$ are the solutions of the system of equations (32).

Another important point to note is the following.

Generally speaking the lift coefficient for an aerofoil or 2-D wing is given by

$$C_l = \frac{dC_l}{d\alpha} \cdot (\alpha - \alpha_0) = C_{l,\alpha} \cdot (\alpha - \alpha_0)$$

The lift curve slope predicted by the inviscid potential flow theory has a value of 2π . However, real flows are viscous and the slope of the linear part of the lift curve of aerofoils in real flows, which can be measured in a wind tunnel test or computed

numerically using a viscous flow CFD software, actually has a value which is somewhat smaller than 2π . In equation (6) it has been assumed that the lift curve slope of the finite wing being analysed has a value of 2π . However, the lifting line equation (8) is not dependent on the choice of the value of the lift curve slope. Therefore, the results that are discussed above have a general validity regardless of whether we use a slope of 2π or slightly less as obtained from wind tunnel testing or computed using viscous CFD software. If the information is available, it is better to use actual viscous lift curve slope values rather than 2π . The lifting line theory does not make any assumption regarding the viscosity of the flowing fluid. It does assume that if the aspect ratio is not too small (larger than 3), the flow over a finite wing may be assumed to be locally 2 dimensional, but it is then corrected slightly by considering the induced velocities at the wing caused by the vortex sheet shed at the trailing edge of the wing. In a true 2 dimensional flow there is no trailing vortex sheet to be considered. A major result that is obtained from the lifting line theory is the prediction of the induced drag, which is associated with the production of lift, not by the action of viscosity. It is predicted that the induced drag is proportional to the square of lift. Furthermore, the lifting line theory also predicts that the induced drag can be minimized by designing the wing (selecting the wing shape) such that the wing load or lift distribution along the span of the wing should approach as closely as possible the ideal elliptic distribution. This can be achieved by manipulating the major parameters of wing aerodynamic design, namely the aspect ratio, the wing planform shape, selection of suitably varying aerofoil cross sections along the span (thus varying the span wise distribution of the zero lift angle of attack) as well as twisting the wing such that the geometric angle of incidence of the aerofoils is not constant but is given by the following equation

$$\alpha(y) = \alpha_{root} + \theta_{twist}(y) \quad (50)$$

There are at least 2 different ways of twisting a finite wing. Firstly, the wing can be twisted along its trailing edge and keeping the leading edge of the wing straight. The other method is to twist the leading edge while keeping the trailing edge level and straight. Since the trailing edge of the wing usually has an attachment, such as flap and aileron, it may be desirable to keep the trailing edge level and straight. In the discussion below it is assumed that the trailing edge is kept level and straight, while the leading edge is twisted such that it is still straight but not level. The conclusion drawn will still be the same, though, if the leading edge is kept level and the trailing edge is twisted.

Consider the initial situation where both the leading and trailing edges are straight and level. The angle of incidences of the aerofoil sections along the span obviously must all be equal, and given the symbol of α_{root} . Initially the leading edge point of any aerofoil must be at the same height as the trailing edge point. If the wing is given a wash out, it means that the wing is twisted such that the leading edge point of the tip aerofoil is now lower than its trailing edge point. Conversely if the wing is given a wash in twist distribution, then the leading edge of the tip aerofoil is now higher than its trailing edge. The trailing edge points remain at the same height, but the leading edge points now are aligned along a straight line, such that the height of any leading edge point relative to its trailing edge point is given by the following equation

$$h(-y) = h(y) = -\frac{2y}{b} \cdot h_{tip} \quad \text{for } -b/2 < y < 0 \quad (51)$$

Now the twist angle, θ_{twist} , is related to $h(y)$ and the aerofoil's chord length as follows

$$\theta_{twist}(-y) = \theta_{twist}(y) = \sin^{-1}\left(\frac{h(-y)}{c(-y)}\right) = \sin^{-1}\left(\frac{2h_{tip}}{b} \cdot \frac{-y}{c(-y)}\right) \quad (52)$$

Note that for a wash out twist the value of h_{tip} is negative, and conversely it is positive for a wash in twist.

In modelling the wing by a bound vortex and a trailing vortex sheet, it was assumed that the bound vortex is a straight line in the span wise direction, normal to the longitudinal direction, and located at the quarter chord line. This imposes a severe restriction on the allowable shape of the wing planform that can be analysed using the LLT (lifting line theory), namely that strictly speaking the wing must not be swept back or swept forward. Any amount of sweepback angle would mean that the bound vortex would now consist of two segments of straight lines, thus at a control point on the left wing we must consider the effect of the right wing segment of the bound vortex and vice versa. This would complicate the resulting lifting line equation considerably. However, it is expected that for a small sweep angle the associated error in neglecting the sweep effect would be small and can be ignored. Any wing planform shape can be analysed using LLT provided that the quarter chord line of the wing is normal or almost normal to the longitudinal axis. This means that the wing to be investigated may have a tapered shape, where the chord length at the wing tip is different (normally smaller) from the chord length at the wing root. It should be noted that in the aerodynamic study of wings, it is always assumed that the fuselage does not exist, such that the two halves of the wing are joined at the plane of symmetry, where $y = 0$. Thus the wing root is located at the plane of symmetry.

A tapered wing normally has a distribution of chord length, which is a linear function of the distance along the wing span. But as far as the LLT method is concerned any kind of span wise distribution of the chord length is quite acceptable as long as the quarter chord line is straight and normal to the longitudinal axis. We shall limit our discussion below to the tapered planform shape where the chord length is distributed linearly, and getting smaller as the tip aerofoil is approached. The chord distribution for such a tapered wing is given by the following equation.

$$c(-y) = c(y) = c_{root} - \frac{c_{tip} - c_{root}}{b/2} y \quad \text{for } -b/2 < y < 0 \quad (53)$$

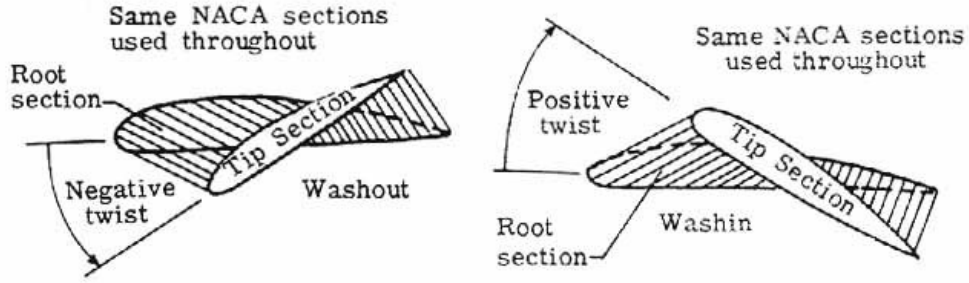
The taper ratio λ is defined as the ratio of the tip chord to the root chord

$$\lambda = \frac{c_{tip}}{c_{root}} \quad (54)$$

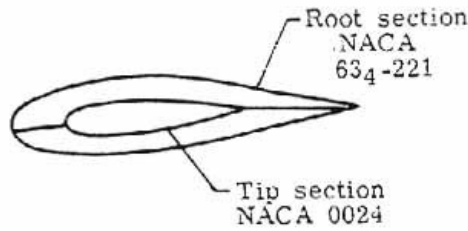
Equation (53) can now be rewritten as follows

$$c(-y) = c(y) = c_{root} \left(1 - \frac{2y}{b} (\lambda - 1)\right) \quad \text{for } -b/2 < y < 0 \quad (55)$$

As well as geometric twist, there is also aerodynamic twist, where the shape of the aerofoil cross section of the wing is smoothly varied, such that the zero lift angle of attack is no longer constant but is a function of span wise distance from the plane of symmetry of the aircraft.



(a) Geometric twist.



(b) Aerodynamic twist.

Geometric and aerodynamic twist.

(Obtained from http://www.centennialofflight.gov/essay/Theories_of_Flight/Reducing_Induced_Drag/TH16G5.htm)

By allowing aerofoil chord, c , geometric angle of incidence, α , and zero angle of incidence, α_0 , to vary along the span wise direction, we must now generalize the Lifting Line Equation (27) for $k = 1, 2, \dots, M$ as follows

$$\frac{2b}{\pi c_k} \sum_{m=1}^M \bar{A}_m \sin(2m-1)\theta_k + \sum_{m=1}^M (2m-1) \bar{A}_m \frac{\sin(2m-1)\theta_k}{\sin\theta_k} = \alpha_k - \alpha_{0,k} \quad (56)$$

The above equation can be written in a more compact form as follows

$$\sum_{m=1}^M C_{km} \bar{A}_m = \alpha_k - \alpha_{0,k} \quad \text{for } k = 1, 2, \dots, M \quad (57)$$

where the matrix coefficient C_{km} is defined as follows

$$C_{km} = \left(\frac{2b}{\pi c_k} + \frac{(2m-1)}{\sin\theta_k} \right) \sin(2m-1)\theta_k \quad (58)$$

$$y_k = -\frac{b}{2} \left(1 - \frac{2k-1}{2M} \right) \quad (59)$$

$$\theta_k = \cos^{-1} \left(\frac{-2y_k}{b} \right) = \cos^{-1} \left(1 - \frac{2k-1}{2M} \right) \quad (60)$$

$$c_k = c(-y_k) = c(y_k) = c_{root} \left(1 - \frac{2y_k}{b} (\lambda - 1) \right) \quad (61)$$

$$\theta_{twist,k} = \sin^{-1} \left(-\frac{2h_{tip}}{b} \cdot \frac{y_k}{c_k} \right) \quad (62)$$

$$\alpha_k = \alpha_{root} + \theta_{twist,k} \quad (63)$$

The variation of the zero angle of attack, α_0 , as a function of y is difficult to be expressed as a simple algebraic equation. The values of α_0 at the wing root and the wing tip must be specified. If the difference of the two angles is quite small, it may be reasonable to assume that $\alpha_0(y)$ can be approximated by a linear relationship.

$$\alpha_{0,k} = \alpha_{0,root} + \left(1 - \frac{2k-1}{2M} \right) (\alpha_{0,tip} - \alpha_{0,root}) \quad (64)$$

The system of equations (57) can be solved simultaneously to calculate the values of the Fourier amplitudes \bar{A}_m for $m = 1, 2, \dots, M$. The wing load per unit span distribution can then be computed for each value of y using the following equation

$$Load(y) = \frac{c(y).C_l(y)}{b} = \frac{2\Gamma(y)}{bV_\infty} = 4 \sum_{m=1}^M \bar{A}_m \cdot \sin((2m-1)\theta(y)) \quad (65)$$

The wing total lift coefficient is given by

$$C_L = \pi \cdot AR \cdot \bar{A}_1 \quad (66)$$

and the induced drag coefficient is given by

$$C_{Di} = \frac{C_L^2}{\pi \cdot AR \cdot e} \quad (67)$$

where the Oswald efficiency factor, e , is computed as follows

$$\delta = \sum_{m=2}^M (2m-1) \left(\frac{\bar{A}_m}{\bar{A}_1} \right)^2 \quad (68)$$

$$e = \frac{1}{1 + \delta} \quad (69)$$

In the above discussion we have taken advantage of the fact that the wing load span wise distribution is symmetrical about the plane of symmetry. The lifting line equation is applied at control points that are all on the left half (port) wing only, or within the range of values of y of $-b/2 < y < 0$. However, because of symmetry the distribution of wing load or lift on the starboard wing can be obtained by simply applying the property of a mirror image, namely $f(y) = f(-y)$.

If the wing load distribution is not symmetrical then we must solve the full lifting line equation (17) rather than the simplified symmetrical version of equation (27). The overall procedure, however, remains basically the same.

Prepared by Hadi Winarto

Last updated 19 May 2004

Please report any typographical and other errors to the author at

Hadi.winarto@rmit.edu.au

Thank you